Crystallization Kinetics of Potassium Sulfate in an MSMPR Agitated Vessel

New data are reported on the crystallization kinetics of potassium sulfate solutions in a laboratory-scale continuous MSMPR cooling crystallizer. Population density distributions determined down to 1 μm by laser light scattering and sieve analysis are corrected for the effects of crystal agglomeration and shape variation and are used to determine accurate growth and nucleation rates. The crystal growth rate is strongly size-dependent, second order with respect to supersaturation, with a high overall activation energy. The surface reaction contribution to the growth process is comparatively large, with a diffusion dependency that increases with crystal size and temperature. While largely consistent with most previous studies, a marked deviation is detected in growth rates at small sizes at which very strong curvature is exhibited in the population density distributions. Secondary nucleation rates vary linearly with suspension density, and the zero size order and activation energy are similar to those of growth but significantly are both much lower at a larger effective size. These observations support the view that growth rate dispersion may be responsible in large part for the substantial variation in reported secondary nucleation kinetics.

A. G. Jones, Jerzy Budz, J. W. Mullin
Department of Chemical and Biochemical Engineering
University College London
London WC1E 7JE, England

Introduction

The crystallization of potassium sulfate from aqueous solution has been the subject of numerous investigations, including those by Mullin and Gaska (1969), Rosen and Hulburt (1971a,b), Ishii (1973), Jones and Mullin (1973), Mullin and Gaska (1973), Garside et al. (1974), Ishii and Fujita (1978), Tavare and Chivate (1979), and Palwe et al. (1984). Although there has been much work, so far there is very little agreement among published data, especially secondary of nucleation rates for which the order with respect to supersaturation varies dramatically from one set of data to another (Randolph and Rajagopal, 1970; Cise and Randolph, 1972; Randolph and Cise, 1972; Randolph and Sikdar, 1976). Recent studies of agglomeration (Budz et al., 1985a) and shape-size dependence of potassium sulfate crystals (Budz et al., 1986b) have shown that both these factors pass through a maximum with crystal size and can contribute to discrepancies in crystallization kinetics determined from the conventional analysis of crystal size distributions (CSD's) from a continuous mixed-suspension, mixed-product-removal (MSMPR) crystallizer.

Correspondence concerning this paper should be addressed to A. G. Jones.

In this present MSMPR study of potassium sulfate crystallization, crystal agglomeration and shape variation were both taken into account for the first time in the analysis of CSD's over a wide range of supersaturation, temperature, and magma density. In addition, use of a Malvern laser light scattering particle sizer facilitated analysis of the population density of very small crystals (down to ~1 μm). Thus the well-known very strong upward curvature of population density vs. size plot could be examined in detail. The crystallization kinetics obtained were then compared with previous work and an attempt made to rationalize the available data.

Theory

Driving force

Proper definition of the driving force of the crystallization process, i.e., supersaturation, σ, is of great importance, especially when temperature-dependent kinetics are to be assessed (Mullin, 1979; Budz et al., 1985b). The fundamental expression of supersaturation is based on activities rather than concentrations (Mullin and Söhnel, 1977). Fortunately, however, for potassium sulfate solutions the error brought about by neglect of activity coefficients is as small as 4% for the highest supersatu-

ration used in crystal growth experiments (Jančić and Grootsholten, 1984). Thus relative supersaturation based on molar, or alternatively mass, units of concentration is acceptable in this work, i.e.:

$$\sigma = \frac{w - w_{eq}}{w_{eq}} \tag{1}$$

where w is the prevailing solution concentration (kg K_2SO_4/kg H_2O) and w_{eq} is the equilibrium solubility.

Linear growth rate

The population density of particles, n, is defined by:

$$n = \lim_{\Delta L \to 0} \left(\frac{\Delta N}{\Delta L} \right) \tag{2}$$

where ΔN is the number of crystals in size range ΔL per unit volume of crystal slurry. The population density can be calculated from the results of any sizing technique by the relation (Mullin, 1972):

$$n_i = \frac{m_i M_T}{\alpha \rho_c L_i^3 \Delta L \sum_i m_i} \tag{3}$$

where m_i is the mass of particles of size L_i, M_T is the magma density, and the subscript i refers to ith size range.

It has been found previously that potassium sulfate crystals exhibit a shape-size dependency (i.e., the volume shape factor, α, varies with crystal size) and agglomeration of the crystals also occurs over a wide size range. Methods for the quantitative assessment of these factors have been reported in detail elsewhere (Budz et al., 1985a, 1986a). Similarly, the growth rate of potassium sulfate crystals is size-dependent (see later). For such size-dependent growth the equation of Sikdar (1977) can be used to calculate growth rates from the CSD:

$$G(L) = \frac{N(L)}{n(L)\tau} \tag{4}$$

where $G(L)$ is the linear growth rate along the characteristic sizing dimension of crystals (in the case of potassium sulfate along the [001] crystallographic axis), $n(L)$ is population density, and τ is the mean residence time within the crystallizer. It should also be noted that the linear growth rates of different faces of potassium sulfate crystals differ (Mullin and Gaska 1973; Budz et al., 1986a).

Several alternative empirical models to describe growth-rate size dependency have been proposed. For example (Bransom, 1960):

$$k_L = aL^c \tag{5}$$

where k_L is the linear growth rate coefficient.
In more generalized form:

$$G/G^o = 1 + aL^c \tag{6}$$

or, alternatively (Abegg et al., 1968):

$$G/G^o = (1 + aL)^c \tag{7}$$

commonly known as the ASL equation.

The dependence of growth rate on supersaturation can be described by the semiempirical equation (Mullin, 1972):

$$G^o = k_G^o \sigma^g \tag{8}$$

It is generally accepted that the growth process consists of two stages (Mullin, 1972; Karpinski, 1985):
Bulk diffusion

$$G_D^o = k_D^o \sigma \tag{9}$$

and
Surface reaction

$$G_R^o = k_R^o \sigma^r \tag{10}$$

The overall growth rate is the combination of these two processes, and the relative contribution of each can vary.

The effect of temperature on the rate constants of these processes may be expressed by an Arrhenius-type relationship (Mullin, 1972):

$$k = k_\infty \exp\left(\frac{-E}{RT} \right) \tag{11}$$

where E is the activation energy for growth (E_G), diffusion (E_D), or reaction (E_R), T is the absolute temperature, and R is the gas constant.

Nucleation rate

It has been found that in many cases a strong upward curvature on a semilog population density-size plot occurs (Randolph and Cise, 1972). In addition to size-dependent growth, such curvature can arise from nuclei distribution and growth rate dispersion. Thus, simple extrapolation to zero size in order to obtain nuclei density, n^o, and subsequently nucleation rate at zero size, i.e.:

$$B^o = n^o G^o \tag{12}$$

becomes uncertain. Alternatively, the effective nucleation rate may be calculated from the equation:

$$B^* = n^* G^* \tag{13}$$

where the superscript* refers to values at the effective size of nuclei L^* (Jančić and Grootscholten, 1984). In this study both approaches are compared.

The nucleation rate in an MSMPR crystallizer is usually correlated by a semiempirical equation of the form (Randolph and Larson, 1971; Garside and Shah, 1980):

$$B = k_N M_T^j \sigma^b \tag{14}$$

or alternatively

$$B = k'_N M_T^j G^i \tag{15}$$

where k_N and k'_N are functions of temperature, hydrodynamics, and impurity concentration.

The temperature effect on nucleation is again usually described by an Arrhenius-type equation (Mullin, 1972):

$$k_N = k_{N,\infty} \exp\left(\frac{-E_N}{RT}\right) \tag{16}$$

The activation energy of nucleation, E_N, has been found to be either positive or negative for different substances (Genck and Larson, 1972; Wey and Terwilliger, 1980; Larson, 1984).

Crystal size distribution

The Malvern particle sizer gives the wt. % values of particles within 16 size bands (L_{M-1}, L_M) where L_M is the diameter of the sphere of the same cross-sectional area as an average projected area of crystals randomly orientated in the laser beam (an average of over 200 individual measurements is taken in each sizing). Before use in a CSD analysis the data must be corrected for crystal agglomeration and shape variation. Crystals of potassium sulfate are approximately parallelepipeds with a width-to-thickness ratio of 2 (Budz et al., 1986a). For such a nonspherical particle shape the Malvern size, L_M, must be recalculated to give the characteristic size, L, corresponding to the crystal width. In this work a procedure proposed by Brown and Felton (1985) was adopted that yielded the relation:

$$L = \left(\frac{\pi}{1 + 6\alpha}\right)^{0.5} \cdot L_M \tag{17}$$

where α is the volumetric shape factor and is size-dependent for potassium sulfate (Budz et al., 1986a). In order to account for crystal shape variation with size, a further recalculation must be made to transform Malvern mass percentage, $m_{i,M}$, into that used in Eq. 3, i.e., m_i. Geometrical considerations lead to the equation:

$$m_i = m_{i,M} \frac{\alpha_i \cdot \sum_i [(1 + 6\alpha_i)^{3/2} L_i^3]}{(1 + 6\alpha_i)^{3/2} \cdot \sum_i \alpha_i L_i^3} \tag{18}$$

Note that for size-independent shape factors $m_i = m_{i,M}$.

The next parameter to be recalculated is the Malvern magma density, $M_{T,M}$, which must be used instead of M_T in Eq. 3. A feature of the Malvern measurement is that the instrument effectively ignores all crystals of sizes larger than its maximum size range. Thus for CSD calculations only the part of magma density should be taken that corresponds to measured size range. This can easily be done by means of the equation:

$$M_{T,M} = M_T(1 - M_k) \tag{19}$$

where M_T is the magma density measured from a mass balance over the crystallizer, and M_k is the cumulative oversize value for size k corresponding to the upper limit of the Malvern range of sizes and is calculated from sieve analysis data. Finally, the effect of agglomeration is accounted for as described previously (Budz et al., 1985a) and the true values of population density vs. size are obtained.

Experimental

The experimental apparatus used is described in detail elsewhere (Budz et al., 1986b). Briefly, it consists of a small laboratory-scale MSMPR crystallizer (capacity 300 mL), double-paddle type stirrer (1,000 rpm), thermostated constant pressure head feed device, flowmeter, and thermostated tank of stock solution pumped to head tanks by means of a peristaltic pump. To determine the crystal size distribution two different techniques were used: standard sieve analysis (50–2,500 μm), and Malvern particle sizer (1–100 μm). The laser particle size analyser facilitated CSD measurement of very small crystals without removal from solution. The entire apparatus was placed in a thermostated chamber permitting the high (up to 40°C) ambient temperatures needed for some experiments. Additional precautionary measures were taken to ensure truly MSMPR conditions. This is especially necessary for potassium sulfate, which produces quite large crystals of relatively high density that are particularly prone to sedimentation. Altogether, 50 individual experiments were carried out over the following ranges of operational parameters:

Relative supersaturation, 0.03–0.16
Magma density, 2–20 kg · m^{-3}
Residence time, 17–59 min
Temperature, 10–50°C

Results

Crystal size distributions

Natural logarithms of population density vs. size for an example run are shown in Figure 1. Malvern and sieve analysis data exhibit an excellent match and support the accuracy of the recalculation procedure adopted. An excellent fit to the data was obtained using an empirical equation of the form:

$$\ln n = P_1 \exp(P_2 L^{0.5} + P_3 L) \tag{20}$$

where P_1, P_2, P_3 are parameters, L is crystal size in μm, and n is population density in m^{-4}. Two curve fits were made. Over the size range 20–800 μm a single correlation was used. However, for extrapolation purposes over the small crystal size range of 4–200 μm shown in the inset of Figure 1, a second correlation was made to cope with the strongly skewed upward curvature. Parameter values are shown in the figure.

Growth rate

The growth rates calculated from Eq. 4 are plotted against size in Figure 2 along with curves for various size-dependent growth models. This will be discussed in detail later. All growth rate data were correlated by combining Eqs. 7, 8, and 11, and the following general equation was obtained:

$$G = 1.44 \exp\left(\frac{-40{,}400}{RT}\right)(1 + 2L^{2/3})\sigma^2 \tag{21}$$

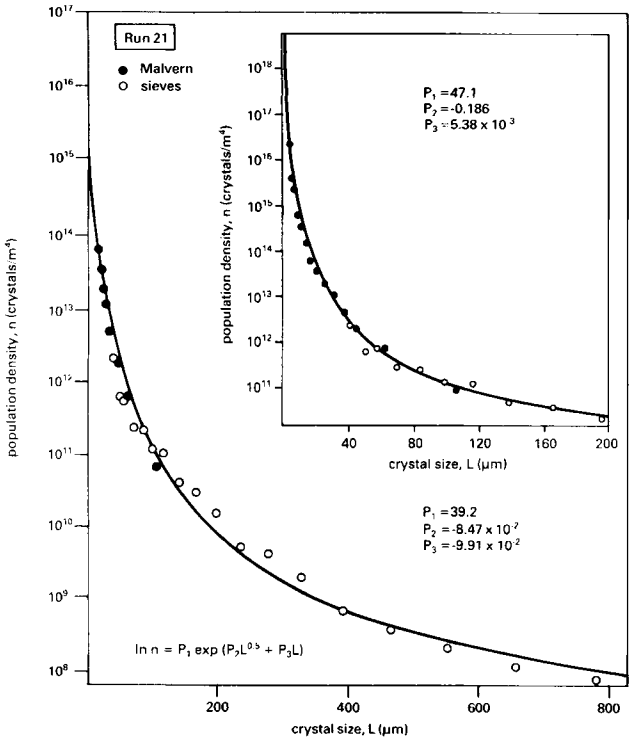

Figure 1. Population density distribution.
——— P_1, P_2, P_3: parameters of Eq. 20
Inset shows small size range

where L is in microns. Equation 21 applies over the range 20–800 μm with an average weighted error of ±25%.

Nucleation rate

Two different methods were used to calculate the nucleation rate, the first using nonlinear extrapolation to zero size to obtain n^o and G^o (employing Eq. 20 over the size range 4–200 μm) and hence B^o from Eq. 12. The second method was based on calculation of the effective nucleation rate, B^*, from Eq. 13. In the latter case an effective size $L^* = 50$ μm was assumed. This corresponds to the smallest crystal beyond the region of sharp upward curvature on the ln n vs L plot and is consistent with previous studies (Gaska, 1966; Jones, 1972). For calculation of n^*, Eq. 20 was used over the size range 20–800 μm and the corresponding value of G^* was obtained from Eq. 21. The nucleation rate data obtained were then correlated by combining Eqs. 14 and 16:

$$B^o = 1.14 \times 10^{24} \exp\left(\frac{-62{,}500}{RT}\right) M_T \sigma^{2.25} \qquad (22)$$

with an average error of ±60%. The fit is comparatively poor due to extrapolation over the small crystal size region.

Correlation of the effective nucleation rate, B^*, yielded the equation:

$$B^* = 2.6 \times 10^{7} \exp\left(\frac{-9{,}300}{RT}\right) M_T \sigma \qquad (23)$$

with an improved average error of ±30%.

Having determined the parameters of Eqs. 21, 22, and 23, it is a simple matter to convert Eqs. 22 and 23 into the form of Eq. 15, whence:

$$B^o = 7.58 \times 10^{23} \exp\left(\frac{-17{,}100}{RT}\right) M_T (G^o)^{1.13} \qquad (22a)$$

and

$$B^* = 4.09 \times 10^{6} \exp\left(\frac{10{,}900}{RT}\right) M_T (G^*)^{0.5} \qquad (23a)$$

It must be pointed out, however, that care should be taken with such transformed equations since the growth rate of hypothetical crystals of zero size has no physical meaning.

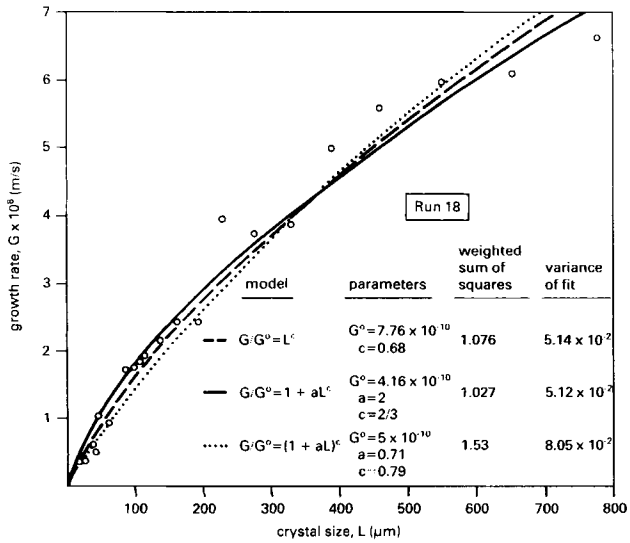

Figure 2. Comparison of various growth models for a representative run.

Discussion

Growth rate

The measured linear growth rate, G in m · s^{-1}, can easily be converted into overall mass rate, R_G in kg · m^{-2} · s^{-1}, using the equation:

$$R_G = \frac{3\alpha\rho_c}{\beta} G \qquad (24)$$

where in this case the volume shape factors α and β ($= 1 + 6\alpha$) are size-dependent (Budz et al., 1986a). This recalculation has been carried out for a selected crystal size (500 μm) and temperature (30°C) for the present data and the values are compared in Figure 3 with corresponding values reported in literature (Mullin and Gaska, 1969; Rosen and Hulburt, 1971a,b; Jones and Mullin, 1973; Garside et al., 1974). When reduced to a common basis, all these data appear highly comparable. In particular, those of Jones and Mullin obtained in a draft-tube agitated vessel (capacity 30 L, marine-type propeller at 550 rpm, and draft tube with four baffles) lie within the range of experimental error (±25%) of the data in the present study. The order of growth is

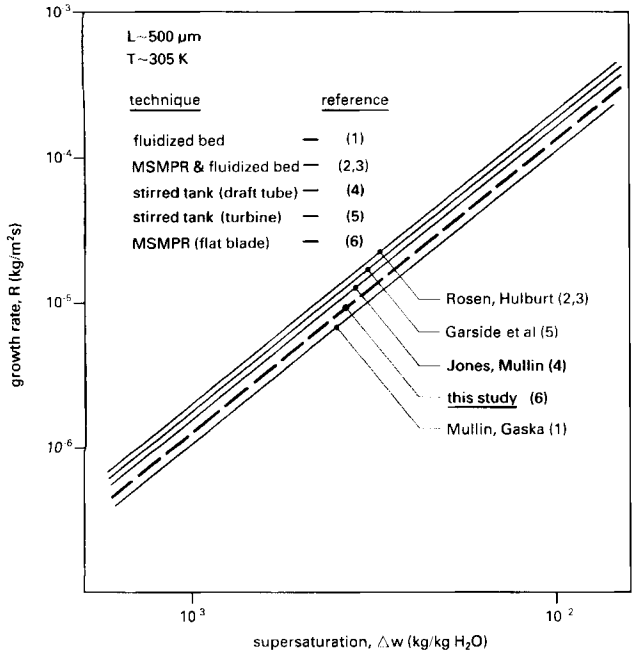

Figure 3. Relative comparison of overall growth kinetics of potassium sulfate crystals.

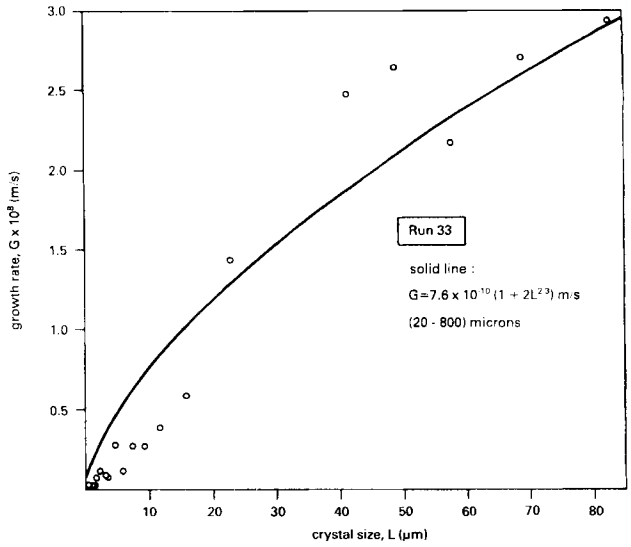

Figure 4. Growth rates of small potassium sulfate crystals.

O calculated, —— extrapolated from larger sizes

equal to 2 in all cases shown although, interestingly, lower orders have been assumed (Ishii, 1973) or determined (Randolph and Rajagopal, 1970; Palwe et al., 1984), indicating a greater apparent diffusion resistance (not shown).

The dependence of the growth rate of potassium sulfate on crystal size has been summarized by White et al. (1976) using data from several sources for either small (2–80 μm) or larger (>100 μm) crystal sizes, which were subsequently combined on the same relative basis. In the present study, crystals sized over the whole range 1–800 μm show almost exactly the same dependence:

$$G = G^o(1 + 2\,L^{2/3}) \tag{25}$$

As yet there is no general agreement on the estimation of the growth rates of crystals smaller than 20 microns. All values calculated using Eq. 25 fall well below model predictions, Figure 4. Thus, size-dependent growth alone does not appear to account for the very high values of population density (low calculated values of growth rate) in the small size range. This deviation is thought to be due to growth rate dispersion.

The growth rate data in this study also suggest a greater size dependence of smaller crystal sizes than of larger ones, Figure 2. For practical purposes, to calculate growth rate of potassium sulfate crystals up to 700 microns Eq. 21 is recommended, whereas for larger crystals the following equation, adopted from a previous study (Jones and Mullin, 1973), is proposed:

$$G = G_{700}(L/700)^{0.5} \tag{26}$$

where G_{700} is the crystal growth rate at 700 μm calculated from Eq. 21 (L in microns).

For the bulk diffusion step of crystal growth (i.e., mass transfer) a reduction in the mass transfer coefficient with increasing crystal size would be expected, despite increasing slip velocity (Nienow, 1969; Lewins and Glastonbury, 1972; Budz et al., 1984) whereas for surface reaction the value of the exponent c in the kinetic equation

$$G = K_R L^c \sigma_R^{2.4} \tag{27}$$

was found to be 0.7 for potassium sulfate (Garside et al., 1974). The comparatively high value of the overall size exponent (0.67) in the present study again suggests that surface reaction offers a much higher resistance to the growth process than diffusion. In order to quantify this phenomenon the concept of the surface integration effectiveness factor, η_R, can be used (Garside et al.):

$$\eta_R = \frac{R_G}{K_R L^c \sigma^{2.4}} \tag{28}$$

The value of η_R at 20°C and for supersaturation $\sigma = 0.10$ was calculated for different crystal sizes using overall growth kinetics found in this study (Eq. 21) and data on surface reaction kinetics of potassium sulfate published in the work of Garside et al. At sizes smaller than 100 μm, Figure 5 shows that the contribution of the surface reaction step to crystal growth process is a decisive one (η_R larger than 0.9). For larger sizes the contribution of bulk diffusion increases slowly, reducing the value of η_R to about 0.7 at 900 μm. It is interesting to note that over the entire size range the surface reaction resistance to the overall growth process is higher than that of bulk diffusion at the supersaturation level most often encountered in practice ($\sigma \sim 0.10$).

The activation energy data that are available for the growth rate of potassium sulfate are in rather poor agreement (Tavare and Chivate, 1979). Generally, however, all reported values of activation energies lie between the limit for bulk diffusion (E_D = 2.4 kJ · mol^{-1}) and that of surface reaction (E_R = 65 kJ · mol^{-1}) (Tavare and Chivate). In the present study, activation energies were recalculated on the basis of relative supersaturation, σ, with concentration expressed as kg salt/kg water. The value obtained (E_G = 40.4 kJ · mol^{-1}) is again in an excellent

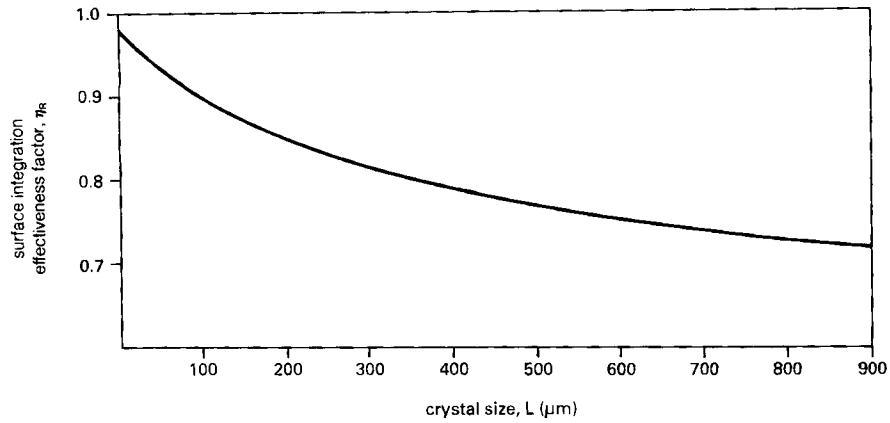

Figure 5. Dependence of surface integration effectiveness factor on crystal size at 20°C for constant supersaturation ($\sigma = 0.10$).

agreement with that reported by Jones and Mullin (1973) (E_G = 39.6 kJ · mol^{-1}, recalculated for σ), and its relatively high value provides further support to the view that the surface reaction contribution is significant. Figure 6 shows effectiveness factors calculated on the basis of the present data of overall growth kinetics (Eq. 21) and those of Garside et al. (1974) of surface reaction kinetics for crystal size L = 710 μm, supersaturation σ = 0.10, at temperatures of 20, 30, 40, and 50°C. As could be expected, the bulk, diffusion contribution increases with increasing temperature, being about 50% at 50°C.

Nucleation rate

Considerable scatter is observed among potassium sulfate nucleation rate data in the literature, even from the same experimental technique. Some of the available data are summarized in Table 1 in terms of the exponents j on magma density and b on supersaturation (Eq. 14). Activation energies are also included where available.

A first-order dependence (i.e., j = 1) is expected for crystal-agitator and crystal-crystallizer collisions and is the most frequently encountered in various systems (Garside and Shah, 1970). The first-order dependency on magma density found in the present study is therefore consistent with theoretical considerations of secondary nucleation but at variance with some other experimental studies.

As shown in Table 1, the published supersaturation orders are also inconsistent. The most probable cause of this variation is the different methods of calculation used in each study. This is clearly shown for values of b found in this work, where two different techniques were used calculation at zero size and at an effective size. For zero-size nuclei the exponent b is substantially higher (2.25) than that (1) for effective nucleation. This indicates that the mechanism responsible for the very large proportion of particles that do not grow to populate the larger size range is also a function of supersaturation and may thus be related to growth rate dispersion, as discussed earlier.

The effect of temperature on secondary nucleation has not been reported as extensively due to the rather limited range of temperatures over which such experiments are possible (Garside and Shah, 1980). From data available in the literature no definite conclusion can be drawn; both negative and positive activation energies have been reported. In the present study the activation energy for zero-size nuclei (reflecting the occurrence of different population events within the small range) is 62.5 kJ · mol^{-1}, which is in very good agreement with the only other available published value (53.3 kJ · mol^{-1}), reported by Randolph and Cise (1972). The zero-size activation energy is thus of the same magnitude as that for growth (40.4 kJ · mol^{-1} for overall

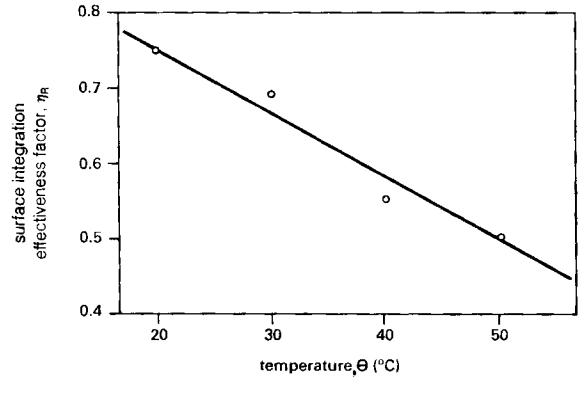

Figure 6. Dependence of surface integration effectiveness factor on temperature.
Crystal size L = 710 μm, supersaturation σ = 0.10.

Table 1. Nucleation Parameters of Potassium Sulfate in an MSMPR Crystallizer

Reference	Exponents, Eq. 14		Activation Energy, E_N^* kJ · mol^{-1}
	Magma Density, j	Supersat., b	
Rosen & Hulburt, 1971a	1	0	—
Randolph & Rajagopal, 1970	0.4	−1	—
Randolph & Cise, 1972	—	0.91	53.3
Randolph & Sikdar, 1976	0.5	0.69	—
This study			
At zero size	1	2.25	62.5
At 50 μm	1	1	9.3

*Supersaturation expressed as σ ($\Delta w/w_{eq}$) with concentration units kg K_2SO_4/kg H_2O.

growth rate and 65 kJ · mol^{-1} for surface reaction only) but significantly is much larger than the effective size activation energy (9.3 kJ · mol^{-1}). This again indicates the possibility of growth rate dispersion occurring within the small size range.

In summary, it can be concluded that potassium sulfate nucleation rate data from an MSMPR crystallizer must be treated with extreme care. Extrapolation to zero size is ambiguous and does not seem to be an accurate method for estimating nucleation rates. In the absence of detailed information of the nuclei distribution and growth dispersion functions in the small size range (<50 μm), the effective nucleation rate currently appears to be the more reliable description of secondary nucleation kinetics.

Acknowledgment

The authors are indebted to the SERC for financial support to undertake this work.

Notation

b = nucleation order
B = nucleation rate, m^{-3} · s^{-1}
c = size-dependent growth model exponent
E = activation energy, kJ · mol^{-1}
g = growth order
G = linear growth rate, m · s^{-1}
i = relative nucleation order
j = exponent of magma density, Eqs. 14, 15
$k, \hat{k}$ = kinetic coefficients, Eqs. 5, 8, 9, 14, 15, 16
L = crystal size (width), m, μm
m = mass, kg
M_k = cumulative mass oversize for kth size band
M_T = magma density, kg · m^{-3}
n = population density, m^{-4}
N = cumulative number oversize, m^{-3}
r = surface reaction order
R = gas constant, 8.3143 J · mol^{-1} · K^{-1}
R_G = mass growth rate, kg · m^{-2} · s^{-1}
T = absolute temperature, K
w = concentration, kgK_2SO_4/kg H_2O

Greek letters

α = volumetric shape factor (i.e., volume = αL^3)
β = surface shape factor (i.e., surface area = βL^2)
Δ = difference
θ = temperature, °C
ρ_c = crystal density, kg · m^{-3}
η_R = surface integration effectiveness factor
σ = supersaturation
Σ = sum
τ = residence time, s

Subscripts

D = diffusion
eq = equilibrium
G = growth
i = size increment
L = linear
M = Malvern data
N = nucleation
R = surface reaction

Superscripts

$*$ = effective size
o = zero size

Literature cited

Abegg, C. F., J. D. Stevens, and M. A. Larson, "Crystal Size Distributions in Continuous Crystallizers when Growth Rate Is Size-dependent," *AIChE J.*, **14,** 188 (1968).

Bransom, S. H., "Factors in the Design of Continuous Crystallizers," *Brit. Chem. Eng.*, **5,** 838 (1960).

Brown, D. J., and P. G. Felton, "Direct Measurement of Concentration and Size for Particles of Different Shapes Using Laser Light Diffraction," *Chem. Eng. Res. Des.*, **63,** 125 (1985).

Budz, J., P. H. Karpinski, and Z. Naruc, "Influence of Hydrodynamics on Crystal Growth and Dissolution in a Fluidized Bed," *AIChE J.*, 30 710 (1984).

Budz, J., A. G. Jones, and J. W. Mullin, "Agglomeration of Potassium Sulfate Crystals in an MSMPR Crystallizer," AIChE Ann. Meet. Chicago (1985a). *AIChE Symp. Ser.* (In press).

Budz, J., P. H. Karpinski, and Z. Naruc, "Effect of Temperature on Crystallization and Dissolution Processes in a Fluidized Bed," *AIChE J.*, **31,** 259 (1985b).

Budz, J., A. G. Jones, and J. W. Mullin, "On Shape-Size Dependence of Potassium Sulfate Crystals," in preparation (1986a).

———, "Effect of Selected Impurities on the Continuous Precipitation of Calcium Sulfate (Gypsum)," *J. Chem. Tech. Biotechnol.*, **36** (1986b).

Cise, M. D., and A. D. Randolph, "Secondary Nucleation of Potassium Sulfate in a Continuous-flow, Seeded Crystallizer," *AIChE Symp. Ser., No. 121,* **68,** 42 (1972).

Garside, J., J. W. Mullin, and S. N. Das, "Growth and Dissolution Kinetics of Potassium Sulfate Crystals in an Agitated Vessel," *Ind. Eng. Chem. Fundam.*, **13,** 299 (1974).

Garside, J., and M. B. Shah, "Crystallization Kinetics from MSMPR Crystallizers," *AIChE J.*, **19,** 509 (1980).

Gaska, C., "Nucleation and Crystallization of Potassium Sulfate," Ph.D. Thesis, Univ. London (1966).

Genck, W. J., and M. A. Larson, "Temperature Effect of Growth and Nucleation Rates in Mixed-Suspension Crystallization," *AIChE Symp. Ser., No. 121,* **68,** 57 (1972).

Ishii, T., "Multiparticle Growth Rates in Vertical Cones," *Chem. Eng. Sci.*, **28,** 1121 (1973).

Ishii, T., and S. Fujita, "Properties of Potassium Sulfate Aqueous Solution and Crystals," *J. Chem. Eng. Data,* **23,** 19 (1978).

Jančić, S. J., and P. A. M. Grootsholten, *Industrial Crystallization,* Delft Univ. Press, Delft (1984).

Jones, A. G., "Programmed Cooling Crystallization of Potassium Sulfate Solutions," Ph.D. Thesis, Univ. London (1972).

Jones, A. G., and J. W. Mullin, "Crystallization Kinetics of Potassium Sulfate in a Draft-tube Agitated Vessel," *Trans. Inst. Chem. Eng.,* **51,** 302 (1973).

Karpinski, P. H., "Importance of the Two-step Crystal Growth Model," *Chem. Eng. Sci.*, **40,** 641 (1985).

Larson, M. A., "Advances in Characterization of Crystal Nucleation," *AIChE Symp. Ser., No. 240,* **80,** 39 (1984).

Lewins, D. M., and J. R. Glastonbury, "Particle-Liquid Hydrodynamics and Mass Transfer in a Stirred Vessel. II: Mass Transfer," *Trans. Inst. Chem. Eng.*, **50,** 132 (1972).

Mullin, J. W., Ed., *Industrial Crystallization 78,* North-Holland Pub., Amsterdam, 93–103 (1979).

———, *Crystallization,* 2nd ed., Butterworths, London (1972).

Mullin, J. W., and C. Gaska, "The Growth and Dissolution of Potassium Sulfate Crystals in a Fluidized-bed Crystallizer," *Can. J. Chem. Eng.*, **47,** 483 (1969).

———, "Potassium Sulfate Crystal Growth Rates in Aqueous Solution," *J. Chem. Eng. Data,* **18,** 217 (1973).

Mullin, J. W., and O. Söhnel, "Expressions of Supersaturation in Crystallization Studies," *Chem. Eng. Sci.*, **32,** 683 (1977).

Nienow, A. W., "Dissolution Mass Transfer in a Turbine-Agitated Baffled Vessel," *Can. J. Chem. Eng.*, **47,** 248 (1969).

Palwe, B. G., M. R. Chivate, and N. S. Tavare, "Growth Kinetics of Potassium Sulfate Crystals in a DTB-Agitated Crystallizer," *Chem. Eng. Sci.*, **39,** 903 (1984).

Randolph, A. D., and M. D. Cise, "Nucleation Kinetics of the Potassium Sulfate-Water System," *AIChE J.*, **18,** 798 (1972).

Randolph, A. D., and M. A. Larson, *Theory of Particulate Processes,* Academic Press, New York-London (1971).

Randolph, A. D., and K. Rajagopal, "Direct Measurement of Crystal Nucleation and Growth Rate Kinetics in a Backmixed Crystal Slurry," *Ind. Eng. Chem. Fundam.*, **9**, 165 (1970).

Randolph, A. D., and S. K. Sikdar, "Creation and Survival of Secondary Crystal Nuclei. The Potassium Sulfate-Water System," *Ind. Eng. Chem. Fundam.*, **15**, 64 (1976).

Rosen, H. N., and H. M. Hulburt, "Continuous Vacuum Crystallization of Potassium Sulfate," *Chem. Eng. Prog. Symp. Ser., No. 110*, **67**, 18 (1971a).

———, "Growth Rate of Potassium Sulfate in a Fluidized-bed Crystallizer," *Chem. Eng. Prog. Symp. Ser., No. 110*, **67**, 27 (1971b).

Sikdar, S. K. "Size-dependent Growth Rate from Curved Log $n(L)$ vs. L Steady State Data," *Ind. Eng. Chem. Fundam.*, **16**, 390 (1977).

Tavare, N. S., and M. R. Chivate, "Growth and Dissolution Kinetics of Potassium Sulfate Crystals in a Fluidized-bed Crystallizer," *Trans. Inst. Chem. Eng.*, **57**, 35 (1979).

Wey, J. S., and J. P. Terwilliger, "Effect of Temperature on Suspension Crystallization Processes," *Chem. Eng. Commun.*, **4**, 297 (1980).

White, E. T., L. L. Bendig, and M. A. Larson, "The Effect of Size on the Growth Rate of Potassium Sulfate Crystals," *AIChE Symp. Ser. No. 153*, **72**, 41 (1976).

Manuscript received Dec. 27, 1985, and revision received June 2, 1986.